



# Multi-finger synergies and the muscular apparatus of the hand

Cristian Cuadra<sup>1,2</sup> · Angelo Bartsch<sup>3</sup> · Paula Tiemann<sup>4</sup> · Sasha Reschechtko<sup>1</sup> · Mark L. Latash<sup>1</sup>

Received: 14 December 2017 / Accepted: 8 March 2018  
© Springer-Verlag GmbH Germany, part of Springer Nature 2018

## Abstract

We explored whether the synergic control of the hand during multi-finger force production tasks depends on the hand muscles involved. Healthy subjects performed accurate force production tasks and targeted force pulses while pressing against loops positioned at the level of fingertips, middle phalanges, and proximal phalanges. This varied the involvement of the extrinsic and intrinsic finger flexors. The framework of the uncontrolled manifold (UCM) hypothesis was used to analyze the structure of inter-trial variance, motor equivalence, and anticipatory synergy adjustments prior to the force pulse in the spaces of finger forces and finger modes (hypothetical finger-specific control signals). Subjects showed larger maximal force magnitudes at the proximal site of force production. There were synergies stabilizing total force during steady-state phases across all three sites of force production; no differences were seen across the sites in indices of structure of variance, motor equivalence, or anticipatory synergy adjustments. Indices of variance, which did not affect the task (within the UCM), correlated with motor equivalent motion between the steady states prior to and after the force pulse; in contrast, variance affecting task performance did not correlate with non-motor equivalent motion. The observations are discussed within the framework of hierarchical control with referent coordinates for salient effectors at each level. The findings suggest that multi-finger synergies are defined at the level of abundant transformation between the low-dimensional hand level and higher dimensional finger level while being relatively immune to transformations between the finger level and muscle level. The results also support the scheme of control with two classes of neural variables that define referent coordinates and gains in back-coupling loops between hierarchical control levels.

**Keywords** Hand · Finger · Synergy · Uncontrolled manifold · Referent coordinate · Motor equivalence · Anticipatory synergy adjustment

## Introduction

The human hand possesses amazing dexterity, which makes even the most sophisticated artificial grippers look clumsy and inept. One of the factors contributing to the hand

dexterity is the ability of the central nervous system (CNS) to ensure stability of salient mechanical variables produced by the digits in a task-specific fashion (cf. Schöner 1995; reviewed in; Zatsiorsky and Latash 2008), an ability which is presumably developed over lifetime (cf. Shaklai et al. 2017). Systems with more elements than constraints (e.g., four fingers producing a prescribed total force) have historically been construed as redundant, leading to the famous problem of motor redundancy (Bernstein 1967), which the CNS must solve by imposing additional constraints or using other computational means, such as optimization, to find unique solutions to motor tasks. In this study, we accept an alternative view that such, apparently redundant, systems are in fact abundant (Latash 2012), i.e., enabling the CNS to facilitate families of solutions that are all able to solve the task. This strategy allows stabilizing salient performance variables in the presence of spontaneous changes in the intrinsic body

---

✉ Mark L. Latash  
mll11@psu.edu

<sup>1</sup> Department of Kinesiology, The Pennsylvania State University, Rec.Hall-267, University Park, PA 16802, USA

<sup>2</sup> Escuela Kinesiología, Facultad de Ciencias de la Rehabilitación, Universidad Andres Bello, Calle Quillota 980, Viña del Mar, Chile

<sup>3</sup> Escuela Kinesiología, Facultad de Medicina, Universidad de Valparaíso, Valparaíso, Chile

<sup>4</sup> Escuela Kinesiología, Facultad de Ciencias de la Salud, Universidad de Viña del Mar, Agua Santa 7075 Rodelillo, Viña del Mar, Chile

states and unexpected changes in the external force field, and performing multiple tasks with the same set of effectors.

Stability of multi-digit action has been studied within the framework of the uncontrolled manifold (UCM) hypothesis (Scholz and Schönner 1999; reviewed in; Latash et al. 2007). This method quantifies two components of inter-trial variance in the space of elemental variables (produced by individual digits): a component that has no effect on a potentially important performance variable, e.g., total force (within the UCM for that variable,  $V_{UCM}$ ), and a component that changes this variable (orthogonal to the UCM,  $V_{ORT}$ ). When both indices are quantified per dimension of their corresponding subspaces, the inequality  $V_{UCM} > V_{ORT}$  indicates that a multi-digit synergy stabilizes the performance variable. Studies of multi-digit synergies have been performed using several different elemental variables including digit forces, moments of force, and finger modes (hypothetical digit-specific variables, Latash et al. 2001; Danion et al. 2004; reviewed in Latash 2008).

Several recent studies linked the idea of multi-digit synergies to a hypothesis on the control of movements with spatial referent coordinates (RCs, Ambike et al. 2016; Reschechtko and Latash 2017). According to this hypothesis, relatively low-dimensional RC for the task-specific performance variables is defined at the highest hierarchical level. Further, a sequence of few-to-many transformations leads to higher dimensional RCs at hierarchically lower levels, e.g., those related to individual digits or individual muscles (Latash 2017). At the muscle level, RC is equivalent to threshold of the tonic stretch reflex ( $\lambda$ ) for the muscle, as in the classical equilibrium-point hypothesis (Feldman 1966, 1986, 2015). According to this theoretical scheme, mapping from RC at the task level to digit-level RC may be independent of the muscle-level organization of the hand action.

The muscle organization of the hand is rather complex. Digits are served with both extrinsic and intrinsic muscles (reviewed in Basmajian and De Luca 1985). Further, many of the involved muscles insert in multiple digits; for example, the multi-digit flexor digitorum profundus (FDP) has four distal tendons inserted at the distal phalanges and the tendons of another multi-digit extrinsic flexor, flexor digitorum superficialis (FDS), insert at the middle phalanges of the fingers. Digit-specific intrinsic muscles produce flexor action with the tendons inserted at the proximal phalanges and contribute to the complex extensor mechanism acting at more distal phalanges (Landsmeer and Long 1965; Long 1965). The different sites of tendon insertion allow testing the effects of this muscular design on multi-finger action; in particular, the role of multi-digit vs. single-digit muscles in the combined action of fingers. A number of earlier studies used a suspension system to vary the involvement of extrinsic and intrinsic muscles in finger force production (Latash et al. 2002; Shinohara et al. 2003). In particular, if a subject

is asked to produce force by the distal phalanges, FDP is the prime mover, while FDS and intrinsic muscles balance the moments in the intermediate joints and help maintain the hand configuration. If force is produced by the proximal phalanges, the roles switch: intrinsic muscles become prime movers while FDP counterbalances the action of the extensor mechanism (Chao et al. 1976; An et al. 1985).

One of the studies compared the performance of maximal voluntary force production (MVC) at the distal and proximal phalanges (Latash et al. 2002). That study quantified indices of finger interaction such as enslaving, defined as unintentional force production by non-instructed fingers when one finger of the hand is instructed to produce force (Zatsiorsky et al. 2000). Note that multi-finger muscles were viewed as a major factor contributing to enslaving (reviewed in Schieber and Santello 2004). The results were unexpected: there were no major differences in indices of enslaving between the two sites of force application. In fact, enslaving was somewhat larger at the proximal phalanges despite the fact that the prime actors were finger-specific intrinsic muscles. Similar to the organization of finger force-stabilizing synergies, there is evidence that enslaving is shaped over a lifetime experience of training because it is lower in musicians (Slobounov et al. 2002) and may be dramatically altered following cortical stroke (Xu et al. 2017).

The main purpose of this study has been to explore whether the neural control of the total force produced by a set of fingers is specific to the muscular organization of the action. Further, our investigation explored whether lifetime experience leads to better force control by the distal phalanges as contrasted with more proximal sites, which are rarely used in ecological tasks. We did this by quantifying finger interaction (enslaving) and coordination (synergies stabilizing total force) while varying the site of force application: at the distal, medial, or proximal phalanges. While the aforementioned study (Latash et al. 2002) suggested that at least some aspects of finger interaction were not crucially dependent on the muscle organization, cadaver studies have suggested that muscle redundancy may be exaggerated in finger force production by showing that losing a single muscle could impose major constraints on performance (Kutch and Valero-Cuevas 2011).

Based on the theory of hierarchical control with RCs, we expected indices of synergies to reflect similar mapping between the RC for total force and individual finger RCs independent of the muscle involvement. So, our first hypothesis was that there would be synergies stabilizing total force at all three sites of force application. On the other hand, force production at the distal site may be viewed as highly practiced, which is not true for force production at the middle and proximal sites. This leads to prediction of higher synergy indices at the distal site (Hypothesis 2). We quantified synergies using finger

forces and finger modes as elemental variables. Using modes removes possible positive co-variation among finger forces due to enslaving. Since stabilization of total force requires predominantly negative co-variation among finger forces (Scholz et al. 2002), we expected the site with larger enslaving (proximal, based on Latash et al. 2002) to show relatively larger synergy indices in the mode space (Hypothesis 3).

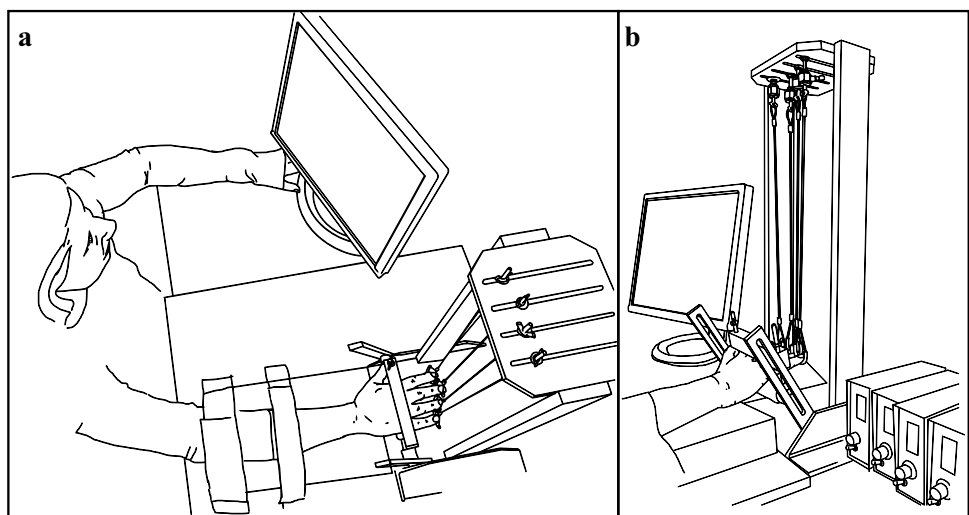
We also explored characteristics of anticipatory synergy adjustments (ASAs, Olafsdottir et al. 2005) defined as a drop in a synergy index in preparation to a quick change in the performance variable. To explore ASAs, subjects were required to produce a very quick force pulse into a target from a steady-state relatively low level of total force. No earlier studies explored ASAs across sites of force application; we, therefore, tentatively hypothesized that ASAs would be larger and longer at the distal site (Hypothesis 4) reflecting the lifetime experience with fingertip force production in contrast to other site of force application.

## Methods

### Subjects

Nine subjects (5 males and 4 females, 26–38 years old, mass  $71 \pm 12$  kg, height  $1.65 \pm 0.05$  m) participated in this study. All subjects self-identified as right-handed according to the preferred hand used during writing and eating. The subjects were healthy, had no history of hand injury or neuromotor disorder, and provided written informed consent in accordance with procedures approved by the Office of Research Protections at The Pennsylvania State University.

**Fig. 1** An illustration of the setup showing the position of the subject, the location of the suspension device, and the monitor used for visual feedback. **a** Top view; **b** side view. Note that the right forearm was fixed with Velcro straps, the hand was fixed allowing only finger action, the fingers were positioned inside the individual loops, and the force sensors were located on top of the suspension system



### Equipment

Four unidirectional piezoelectric sensors (model 208C02, PCB Piezotronics, Depew, NY) were used to measure the force produced by individual fingers. The sensors were attached with threaded rods to the slots in the top plate of the frame of the experimental device (suspension device, Fig. 1a). This configuration allowed vertical adjustments in a range of 40 mm. The slots were placed 30 mm apart in the mediolateral direction and allowed adjustments in the finger longitudinal direction in a range of 150 mm. Both vertical and longitudinal adjustments could be made to accommodate individual differences in finger anatomy. A loop of aircraft cable was suspended from each sensor; the bottom end of the loop was covered in rubber to allow for comfortable finger placement. A hand fixation system was used to stabilize the palm of the hand to ensure a constant hand configuration throughout the experiment (Fig. 1b). A 20" monitor was located 0.6 m from the subject's head at eye level, to set tasks and provide visual feedback on their performance.

The signals from each sensor were sent through a signal conditioner (PCB, model 484B06) to a 16-bit analog-to-digital converter (BNC 2110; National Instruments). A LabVIEW-based software (National Instruments, Austin, TX) was developed to display visual feedback and record the force signals from individual fingers at 1000 Hz.

### Procedure

The subjects were seated in a chair facing the testing table with his/her right upper arm at approximately  $45^\circ$  of abduction in the frontal plane,  $45^\circ$  of flexion in the sagittal plane and the elbow at approximately  $45^\circ$  of flexion. The forearm was fixed by Velcro straps flat on the supporting surface that was at the same height as the support point of the hand

fixation device. The wrist was at 20° of extension. The metacarpophalangeal (MCP) joints were at 20° (Fig. 1b). The loops were positioned against the middle part of the finger's phalanx tested; there were three sites of force application with the loops positioned against the proximal phalanges, PP; middle phalanges, MP; and distal phalanges, DP. The left hand rested on the table.

The experiment involved four tasks performed under each of the three site conditions (PP, MP and DP). The four tasks were performed in blocks for each of the conditions, while the conditions were performed in a random order across participants. The complete experiment was performed on the same day for each subject; it lasted about 1 h and 10 min.

### Maximal voluntary contraction (MVC) task

The subjects were instructed to press on the loops attached to the sensors with the four fingers together as hard as possible in a self-paced manner during 4 s. The sum of the four fingers forces ( $F_{TOT}$ ) was shown on the screen. Three trials were performed with 30-s relaxation periods. The highest MVC total force ( $F_{MVC}$ ) across the three trials was used to normalize the following tasks.

### Single-finger ramp task

Subjects were asked to press on the loops with one of the four fingers (task-finger) and match a force template shown on the screen that represented the task-finger  $MVC_i$ -normalized force profile from 5 to 40% ( $i$ : Index, Middle, Ring or Little). Each single-finger ramp trial lasted 10 s. The first 3 s consisted of a horizontal segment at 5% of  $MVC_i$ , followed by 5 s of a slanted line from 5 to 40% of  $MVC_i$ , and then 2 s at 40% of  $MVC_i$ . Subjects were required to press with the task finger while keeping all the fingers on the loops and not paying attention to possible force produced by the non-task fingers. Subjects had three practice trials before the data were collected. Trials in which the subjects lifted up a non-task finger from the loops were discarded and repeated. This task was used to convert and analyze finger forces in mode space (See “Data analysis”).

### Force-pulse task

In the force-pulse task, subjects pressed with all fingers to produce the required total force ( $F_{TOT}$ ) time profile. They were asked to produce a steady  $F_{TOT}$  level at 5% of  $F_{MVC}$ ; then, at any time after 6.75 s had elapsed from the beginning of the trial, they were asked to produce a pulse into a target set at  $0.25 \pm 0.05$  of  $F_{MVC}$ . This time was identified on the screen with a vertical line and served as a cue that they could produce a force pulse at any time in a

self-paced manner. This time was chosen to allow subjects to have enough time to stabilize  $F_{TOT}$  before initiating a pulse, while giving them enough time to self-initiate the pulse without being rushed by the impending end of the trial. The target force window was shown on the screen as two horizontal lines, which represented an interval between 0.2 and 0.3 of  $F_{MVC}$ . After they produced a force pulse, subjects were instructed to return to the initial steady-state force level as quickly as possible. For the entire duration of each trial, subjects received visual feedback on  $F_{TOT}$ . The instruction emphasized accuracy of  $F_{TOT}$  performance during steady-state phases, not making counter-movements before the force pulse, and trying to land the  $F_{TOT}$  peak on the target. This task was used to analyze the structure of variance before and after the pulse in multi-finger synergies stabilizing the  $F_{TOT}$ .

The trials that did not fulfill the listed requirements and trials with slow force pulses ( $> 0.5$  s) were rejected and repeated. The subjects performed 24 trials. Before experimental trials, subjects practiced the task for about 3 min.

### Steady-state task

During this task, subjects were instructed to press with all the fingers and match  $F_{TOT}$  to a visual target set at 0.2 of  $F_{MVC}$ ; after 6 s, the cursor disappeared and subjects were instructed to continue producing the same force for the remainder of the trial (approximately 20 s). Five trials were recorded after three practice trials. The purpose of this task was to explore force stability using indices of unintentional force drop typically seen after turning the visual feedback off (Vaillancourt and Russell 2002; Ambike et al. 2015).

### Data analysis

Data were processed off-line using routines written in MATLAB R2016a (The Mathworks, Natick, MA). Before analysis, data were low-pass filtered using a zero-lag fourth-order Butterworth filter with a cutoff frequency of 10 Hz.

### MVC and single-finger ramp tasks

The MVC was computed at the time where  $F_{TOT}$  reached maximum during the trial. The enslaving matrix ( $\mathbf{E}$ ) reflects the unintentional forces produced by non-task fingers during the single-finger ramp task (Zatsiorsky et al. 1998; 2000). A 3-s time interval was used, starting 1 s after the ramp initiation and 1 s before ramp termination to avoid edge effect. The regression coefficients from (Eq. 1) were used to construct  $\mathbf{E}$ :

$$F_{i,j} = f_i^0 + k_{i,j} \cdot F_{TOT,j} \quad (1)$$

$$\mathbf{E} = \begin{bmatrix} k_{I,I} & k_{I,M} & k_{I,R} & k_{I,L} \\ k_{M,I} & k_{M,M} & k_{M,R} & k_{M,L} \\ k_{R,I} & k_{R,M} & k_{R,R} & k_{R,L} \\ k_{L,I} & k_{L,M} & k_{L,R} & k_{L,L} \end{bmatrix},$$

where  $i, j = \{I, M, R, L\}$ ,  $j$  represents the task finger;  $F_{ij}$  indicates the individual  $i$ -finger force when the  $j$ -finger was pressing, and  $F_{TOT,j}$  is the total force when the  $j$ -finger was pressing. To compare  $\mathbf{E}$  across the three sites (PP, MP, and DP) and across fingers, we computed an enslaving index ( $\mathbf{E}_{Nj}$ ) as the sum of all the non-diagonal elements of  $\mathbf{E}$  for each task finger. We also computed the average of all non-diagonal elements in  $\mathbf{E}$  ( $\mathbf{E}_{AV}$ ).

### The force-pulse task

Despite the trial acceptance criteria applied during data acquisition (described earlier), some unacceptable trials were collected. During the off-line processing, trials were rejected based on the following criteria: visible counter-movement prior to the pulse, multiple peaks during the pulse, and pulse duration > 0.5 s. All of the accepted trials (83% overall) were aligned based on the point when the time derivative of  $F_{TOT}$  exceeded 5% of its maximal value during the trial ( $t_0$ ). The performance of the force-pulse task was described with the peak force ( $F_{PEAK}$ ) as the maximal  $F_{TOT}$  recorded during the trial, and the time of the peak ( $t_{PEAK}$ ) from  $t_0$  to the time where  $F_{PEAK}$  was observed.

### Analysis of the structure of variance

The analysis of multi-finger synergies stabilizing the  $F_{TOT}$  profile was performed within the framework of the UCM hypothesis (Scholz and Schöner 1999; reviewed in; Latash et al. 2007). According to this hypothesis, the CNS manipulates a set of elemental variables, finger forces or finger modes (hypothetical commands to fingers, Danion et al. 2003), to stabilize  $F_{TOT}$ . Inter-trial variance of the elemental variables (finger modes) across the attempts was partitioned into two components, one within the UCM ( $V_{UCM}$ ; which does not affect  $F_{TOT}$ ) and another orthogonal to it ( $V_{ORT}$ ; which affects  $F_{TOT}$ ). If the elemental variables are indeed organized into a synergy stabilizing  $F_{TOT}$ ,  $V_{ORT}$  is expected to be significantly smaller as compared to  $V_{UCM}$ , after both are quantified per dimension in the corresponding spaces.

The enslaving matrix  $\mathbf{E}$  was used to convert the  $4 \times 1$  force data vector  $\mathbf{f}$  ( $\mathbf{f} = [f_I, f_M, f_R, f_L]^T$ ) into a set of finger modes:  $\mathbf{m} = \mathbf{E}^{-1}\mathbf{f}$  where  $\mathbf{m}$  is the  $4 \times 1$  mode vector for each sample.

We performed further analyses in two spaces, forces ( $f$ ) and modes ( $m$ ). Variance across trials was computed for each time sample, and compared within the two subspaces, UCM

and ORT. Each value was normalized per dimension in the corresponding space. The index of synergy ( $\Delta V$ ) was computed to measure the amount of  $V_{UCM}$  in the total variance ( $V_{TOT}$ ):

$$\Delta V = \frac{V_{UCM}/3 - V_{ORT}/1}{V_{TOT}/4}. \tag{2}$$

A Fisher's z-transformation of  $\Delta V$  values was performed adapting to the constrained boundaries of  $\Delta V$ :  $[-4, 1.33]$ . This transformation was done prior to applying parametric statistical analysis (Solnik et al. 2013):

$$\Delta V_z = 0.5 \log \frac{(4 + \Delta V)}{(1.33 - \Delta V)}, \tag{3}$$

For the steady-state (SS) analysis before the force pulse, a 0.5-s time window was used from  $-1.5$  s to  $-1.0$  s prior to  $t_0$ . Averages and standard deviations (SD) were computed for  $\Delta V_z$ ,  $V_{UCM}$  and  $V_{ORT}$ .  $V_{UCM}$  and  $V_{ORT}$  were normalized by  $F_{MVC}^2$  per degree-of-freedom.

### Analysis of anticipatory synergy adjustments (ASAs)

ASAs were identified as a drop in  $\Delta V_z$  time profile prior to  $t_0$ . We computed the time of ASA onset ( $t_{ASA}$ ) as the instant when  $\Delta V_z$  decreased by one SD below the average value over the SS and stayed below that average value until  $t_0$ . Changes in the index of synergy ( $\Delta \Delta V_z$ ) and variance indices ( $\Delta V_{UCM}$  and  $\Delta V_{ORT}$ ) over the ASA were computed as the differences between the values during SS and  $t_0$ . In cases where  $\Delta V_z$  did not drop by one SD before  $t_0$ , both  $t_{ASA}$  and  $\Delta \Delta V_z$  were defined as 0 (this happened in only one subject).

### Motor equivalence analysis

The motor equivalence analysis quantified two components of displacement in the spaces of finger forces and modes from the pre-pulse steady state to the post-pulse steady state. The first component preserved  $F_{TOT}$  (motor equivalent,  $ME$ ), while the second led to a change in  $F_{TOT}$  (non-motor equivalent,  $nME$ ). We computed the difference in individual finger forces ( $\Delta f$ ) between the pre-pulse steady state and a 0.5-s time window 2 s after the pulse initiation (defined as the post-pulse steady state). The  $\Delta f$  values were projected onto the UCM to compute the  $ME$ , and onto the ORT to compute the  $nME$  component. Both quantities were normalized by the square root of dimensionality of the corresponding spaces (Mattos et al. 2011).

## Steady-state task

To quantify the unintentional force drifts caused by turning the visual feedback off, we averaged  $F_{TOT}$  over the five trials and computed the drift magnitude ( $\Delta F_{TOT}$ ) as the difference between two 1-s windows, just after the time when visual feedback was removed and just before the trial end. These values were normalized with respect to the task magnitude and converted into normalized force units, NFU:  $F(NFU) = F(N)/0.2F_{MVC}(N)$  for across-site and across-subject comparisons.

## Statistics

Descriptive statistics are reported in the text and figures as means  $\pm$  standard error (SE), unless otherwise stated. Most of the analysis described below was performed twice, in the force and mode spaces. Repeated-measures ANOVA procedure was used to test all the hypotheses at  $p < 0.05$ . To compare the MVC and the enslaving indices,  $E_{AVG}$  and  $E_N$ , across the three sites of force application, a one-way ANOVA was used (Site, three levels: PP, MP, and DP). In addition, enslaving was compared across fingers with a two-way ANOVA Site  $\times$  Finger (four levels: I, M, R, L). To explore synergy indices during pre-pulse steady state, a one-way ANOVA was performed for  $\Delta V_Z$  and a two-way ANOVA for variance indices, Site  $\times$  Space (two levels: UCM and ORT). To explore indices of ASAs, a one-way ANOVA was used (Site) on  $\Delta \Delta V_Z$  and  $t_{ASA}$ . To explore the force-pulse performance,  $F_{PEAK}$  and  $t_{PEAK}$  were compared using a one-way ANOVA (Site). For motor equivalence analysis, a two-way ANOVA was used (Site  $\times$  Space). To explore the relation between  $\sqrt{V_{UCM}}$  versus  $ME$ , and  $\sqrt{V_{ORT}}$  versus  $nME$ , Pearson correlation analysis was used. Finally, to compare the unintentional drift in forces we used a one-way ANOVA (Site) on  $\Delta F_{TOT}$  in both force and mode spaces. Bonferroni corrections were used to explore significance of pairwise contrasts. Normality assumptions were inspected with the  $qq$ -plot. All the statistical analyses were performed with SAS 9.4 (The SAS Institute, Cary, NC) and MATLAB.

## Results

The subjects produced higher peak forces in the MVC tasks when they pressed with the proximal phalanges. On average, the MVC magnitude was at PP  $107.06 \pm 12.87$  N, at MP  $78.15 \pm 11.33$  N, and at DP  $89.90 \pm 15.32$  N ( $F_{[2,16]} = 9.23$ ;  $p < 0.05$ ). Pairwise comparisons confirmed significant differences between the PP and MP sites ( $t_{[16]} = -29.90$ ;  $p < 0.01$ ).

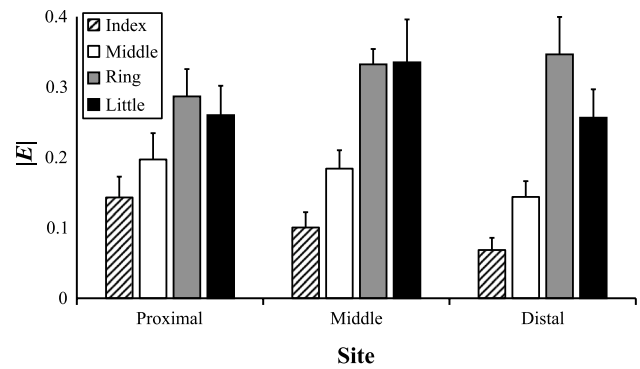


**Fig. 2** The index of enslaving,  $E_N$ , computed for individual fingers during force production by different phalanges (sites). Mean data across subjects are shown with SE bars. Note the similarities in the  $E_N$  values across sites. The Index finger showed the smaller  $E_N$  and the Ring finger showed the highest  $E_N$

Analysis of unintentional force production by non-task fingers (enslaving) did not show significant differences for  $E_{AVG}$  across the three sites (PP:  $0.074 \pm 0.008$ , MP:  $0.081 \pm 0.007$ , and DP:  $0.069 \pm 0.007$ ;  $F_{[2,16]} = 1.14$ ;  $p > 0.05$ ). There were, however, significant differences across the fingers reflected in different magnitudes of  $E_N$  (I:  $0.104 \pm 0.014$ , M:  $0.175 \pm 0.016$ , R:  $0.321 \pm 0.025$ , and L:  $0.283 \pm 0.027$ ;  $F_{[3,88]} = 22.72$ ;  $p < 0.001$ ). In particular, the I finger showed the lowest enslaving while the R finger showed the largest enslaving indices. Analysis of  $E_N$  showed no difference across the three sites and no Site  $\times$  Finger interaction. Pairwise comparisons confirmed  $I < R, L$  and  $M < R, L$  ( $p < 0.05$ ). These results are illustrated in Fig. 2, which shows averaged across subjects  $E_N$  for each finger and each site of force application.

Analysis of the two components of inter-trial variance,  $V_{UCM}$  and  $V_{ORT}$ , during the pre-pulse steady state showed  $V_{UCM} > V_{ORT}$  across all three sites in both force space and mode space ( $F_{[1,40]} > 29.0$ ;  $p < 0.001$ ). There were no significant differences across the three sites and no Site  $\times$  Space interaction (Fig. 3a). Correspondingly, the index of synergy  $\Delta V_Z$  was always higher than the critical value of 0.55 and showed no significant differences across the three sites either in the force space (PP:  $1.469 \pm 0.097$ , MP:  $1.581 \pm 0.101$ , and DP:  $1.448 \pm 0.138$ ) or in the mode space (PP:  $1.815 \pm 0.141$ , MP:  $2.056 \pm 0.131$ , and DP:  $1.804 \pm 0.178$ ).

Characteristics of the force pulse, such as  $F_{PEAK}$  and  $t_{PEAK}$ , were similar across the three sites. On average,  $F_{PEAK}$ , normalized by MVC force, was  $0.341 \pm 0.028$  norm, and  $t_{PEAK}$  was  $0.132 \pm 0.007$  s. Prior to the force pulse, there was a consistent drop in the synergy index (anticipatory synergy adjustments, ASAs), which started about 0.150–0.250 s prior to the force pulse initiation. Figure 4 illustrates the force pulse and  $\Delta V_Z$  changes for a representative subject. The timing of ASAs,  $t_{ASA}$ , showed no significant

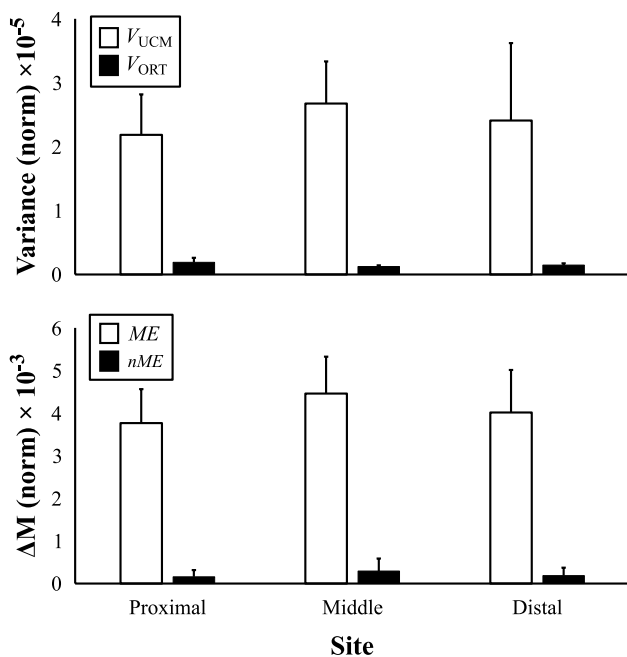
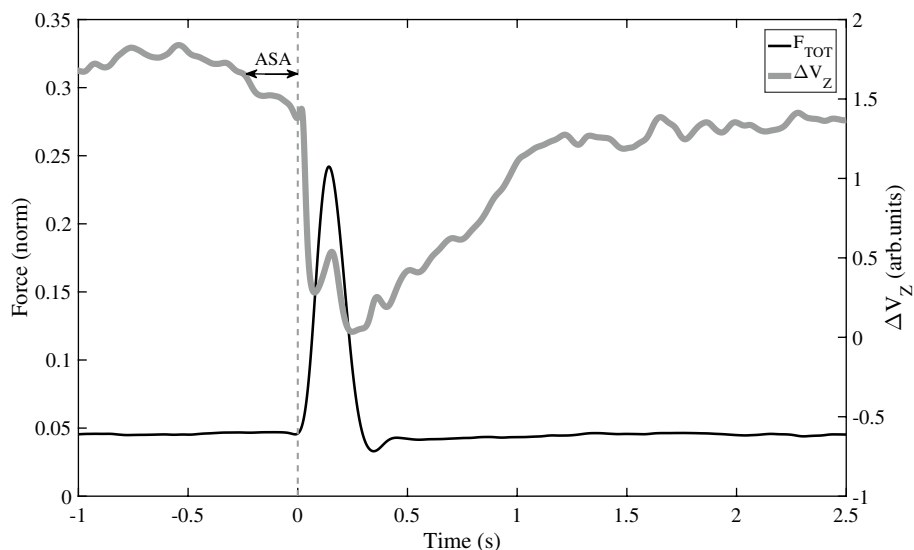


**Fig. 3** Indices of the inter-trial variance analysis,  $V_{UCM}$  and  $V_{ORT}$  (a normalized by  $F_{MVC}^2$ , per degree-of-freedom), and of motor equivalence analysis,  $ME$  and  $nME$  (b normalized by  $F_{MVC}$ , per square root of degrees-of-freedom). All indices were computed using finger modes (similar results were obtained for analysis in the finger force space). Averaged across subjects data with standard error bars are shown. Note that across the three sites of force application,  $V_{UCM} > V_{ORT}$  and  $ME > nME$

differences across the three sites for analysis in both force space (PP:  $0.242 \pm 0.104$  s, MP:  $0.182 \pm 0.087$  s, and DP:  $0.170 \pm 0.064$  s) and mode space (PP:  $0.243 \pm 0.104$  s, MP:  $0.180 \pm 0.088$  s, and DP:  $0.168 \pm 0.064$  s). The data of one subject were removed from this analysis because his  $t_{ASA}$  values were  $> 3$  standard deviations above the mean across

**Fig. 4** Typical performance in the force-pulse trial by a representative subject for the distal site of force application. Total force,  $F_{TOT}$  (black solid line, in fractions of MVC) and the synergy index,  $\Delta V_Z$  (solid gray line) are shown. Anticipatory synergy adjustment (ASA) is shown with the double-sided arrow



all three sites. The magnitude of the drop in  $\Delta V_Z$  during the ASAs also did not differ across the sites and was similar for the analysis in the force (PP:  $0.571 \pm 0.116$ , MP:  $0.568 \pm 0.154$ , and DP:  $0.414 \pm 0.147$ ) and mode space (PP:  $0.521 \pm 0.117$ , MP:  $0.568 \pm 0.154$ , and DP:  $0.414 \pm 0.146$ ).

Comparisons of displacements within the UCM ( $ME$ ) and within ORT ( $nME$ ) spaces between the pre-pulse and post-pulse steady states showed similar magnitudes for analysis of finger forces and modes. These data are illustrated in Fig. 3b. Across the three sites,  $ME > nME$  ( $F_{[1,40]} = 14.93$ ;  $p < 0.001$ ), without effect of Site and without an interaction.

There was significant correlation across subjects between  $ME$  and  $\sqrt{V_{UCM}}$  for all three sites (PP:  $R = 0.7875$ , MP:  $R = 0.7412$ , DP:  $R = 0.8565$ ;  $p < 0.01$ ). However, there were only weak correlations between  $nME$  and  $\sqrt{V_{ORT}}$  for all sites (PP:  $R = 0.3886$ , MP:  $R = 0.2254$ , DP:  $R = 0.4244$ ;  $p > 0.1$ ).

Turning visual feedback off led to a slow drift in  $F_{TOT}$  to lower magnitudes. The drift was observed across all sites but its magnitude differed across the three sites (PP:  $-0.165 \pm 0.029$  norm, MP:  $-0.190 \pm 0.032$  norm, and DP:  $-0.128 \pm 0.025$  norm;  $F_{[2,16]} = 3.98$ ;  $p < 0.05$ ). Pairwise comparisons confirmed a significant difference between the DP and MP sites ( $p < 0.05$ ).

## Discussion

Only one of our specific hypotheses has been supported by the data. Indeed, we saw strong synergies stabilizing total force at all three sites of force application, reflected in the inequality  $V_{UCM} > V_{ORT}$  leading to indices of synergy  $\Delta V > 0$  (cf. Hypothesis 1). While this result was expected based on earlier studies of synergies during multi-finger force production at the fingertips (Latash et al. 2001; Scholz et al. 2002), it was not trivial with respect to the two unusual tasks with

force production at the middle and proximal phalanges. All other specific hypotheses have been falsified. In particular, we saw only minor differences in MVC force and force drift magnitude, while no differences were seen for other variables among the three sites of force application (cf. Hypothesis 2) and no site-related differences between the results of analysis in the force and mode spaces (cf. Hypothesis 3). The only difference between the two spaces was expected: Synergy indices were higher in the mode space analysis compared to the force space analysis due to the removal of positive finger force co-variation (enslaving, Zatsiorsky et al. 2000) in the former analysis. Our tentative hypothesis related to anticipatory synergy adjustments (ASAs, Olafsdottir et al. 2005; Shim et al. 2005) has been also falsified (cf. Hypothesis 4). We saw no significant differences in the ASA timing ( $t_{ASA}$ ) and magnitude ( $\Delta\Delta V_Z$ ) across the three sites of force production. There were signs of slightly lower  $F_{TOT}$  stability and smaller ASAs for the tasks performed at the distal phalanges (which go against our Hypotheses 2 and 4). Only one comparison, however, reached significance: the force drift in the trials without visual feedback was larger for the DP site compared to the MP site. Given that other comparisons failed to reach significance, we view this effect as small and, at this time, prefer not to speculate on its origins. Further, we discuss implications of these results for the scheme of hierarchical control with referent coordinates (RCs; cf. Latash 2010; Feldman 2015), for issues of muscle-level control, and for the possible role of lifetime experience in shaping finger coordination.

### Hierarchical control of the hand with referent coordinates

We accept in this paper a theory of motor control that is based on physics and physiology (reviewed in Latash 2016, 2017). According to this theory, the neural control process can be adequately described with setting parameters (referent coordinates for effectors, RCs) for laws of nature that define interactions among subsystems within the organism and between the organism and the environment. Performance variables—kinetic, kinematic, and electromyographic—emerge without being pre-computed by the CNS. Within this general scheme, force production by a set of fingers may be viewed as a control hierarchy involving three levels. At the highest level (Task level in Fig. 5), a time profile of RC for the hand is defined ( $RC_{TASK}$ ).

Further, two abundant transformations take place. First  $RC_{TASK}$  leads to RCs at the individual finger level ( $RC_{FINGER}$ ). Then, each  $RC_{FINGER}$  leads to RCs for all the involved muscles (and muscle compartments); these RCs are equivalent to thresholds for stretch reflex ( $\lambda$ ) as in the classical equilibrium-point hypothesis (Feldman 1966, 1986). For simplicity, in this description we assume that

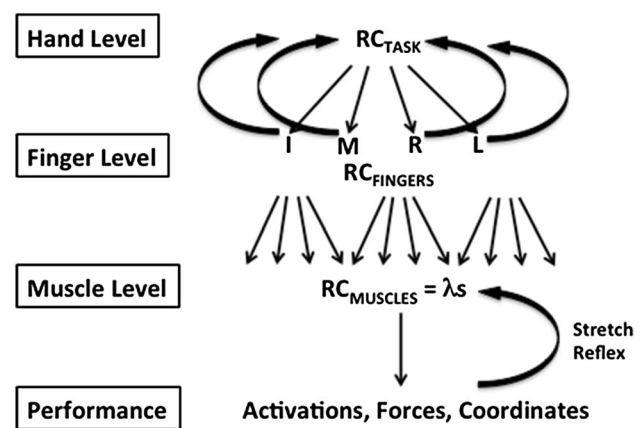


**Fig. 5** An illustration of a hypothetical control hierarchy involving three levels. At the highest level (Hand level), a time profile of the hand referent coordinate is defined ( $RC_{TASK}$ ). Two abundant transformations are assumed. First,  $RC_{TASK}$  leads to RCs at the individual finger level ( $RC_{FINGER}$ ). Then, each  $RC_{FINGER}$  leads to RCs for all the involved muscles (and muscle compartments), which are equivalent to their thresholds for stretch reflex ( $\lambda$ ). Muscle activations and finger forces emerge given the hand configuration and external resistance. Feedback loops between the levels are assumed (illustrated for the Hand-to-Fingers transformation)

the current coordinate of each of the effectors is zero. This is valid for isometric tasks while the description has to be adjusted for tasks involving motion of the effectors. In addition, this scheme does not distinguish between the two basic commands,  $r$ -command and  $c$ -command (Feldman 1980, 1986), which can be introduced at any level of analysis. In particular, the  $c$ -command defines the spatial range where opposing muscle groups can be active simultaneously. This command leads to effective changes in apparent stiffness (Latash and Zatsiorsky 1993) of the effector controlled by those muscle groups.

Two abundant (few-to-many) transformations are illustrated in Fig. 5. According to the principle of abundance (Gelfand and Latash 1998; Latash 2012), such transformations are organized in a synergic way, i.e. they stabilize a salient performance variable while allowing flexible involvement of the elements. This may be achieved, in particular, by back-coupling feedback loops between the levels (as in Latash et al. 2005; Martin et al. 2009). In our experiment, the task was always the same and the set of fingers was also unchanged. So, it is safe to assume that the first transformation, Task-to-Fingers, was common among the three sites of force application. In contrast, the muscle involvement was different for the three sites suggesting that the second transformation, Finger-to-Muscles, differed across the three conditions.

Our finding of comparably strong synergies stabilizing total force across the three sites of force application suggests that such synergies were primarily defined by the

Task-to-Fingers transformation common across the conditions. We expected synergies to be stronger for the distal site of force application reflecting the lifetime practice of similar tasks, while force application by the proximal and middle phalanges is rather unusual. This expectation was not supported by the data; actually all the differences between the means were in the direction of smaller indices for the DP condition. Assuming that practice defines synergy indices (cf. Domkin et al. 2002; Kang et al. 2004; Wu and Latash 2014), the findings suggest that lifetime experience affected only the Task-to-Fingers part of the hierarchy in Fig. 5, while the Finger-to-Muscles transformation may be viewed as immune to effects of practice. It is possible that such low-level transformations are robust across muscle groups. This conclusion fits well the classical statement: “The brain knows nothing about muscles; it knows only movements” by Hughlings Jackson (1889). An example of such synergic transformation is the system of Renshaw cells that may be viewed as a mechanism stabilizing the output of a motoneuronal pool to a muscle consisting of numerous motor units (Latash et al. 2005). It is possible that prolonged specialized training can lead to changes in the Finger-to-Muscle transformations, e.g., in professional musicians (cf. Slobounov et al. 2002). Note, however, that our subjects did not have specialized hand training.

The last conclusion seems at odds with results of a modeling study by Kutch and Valero-Cuevas (2011) showing that muscle redundancy may be exaggerated. That study has shown that removing a single muscle from an apparently redundant set prevents the system from performing certain tasks. We would like to emphasize here the difference between accessible task space and stability within that space. The principle of motor abundance addresses the latter aspect of functioning of an apparently redundant system but not the former one.

### What is the role of different muscle involvement?

Force production at different finger phalanges is expected to lead to different muscle involvement (Landsmeer and Long 1965; Long 1965; Darling et al. 1994; Basmajian and DeLuca 1985). In particular, during pressing with the fingertips, the FDP is the prime mover while FDS and intrinsic muscles participate in balancing moments in intermediate finger joints; in addition, the intrinsic muscles play the role of antagonists via the extensor mechanism (Li et al. 2000, 2002). During pressing at middle phalanges, the FDS is the prime mover, while intrinsic muscles produce flexion moment at the metacarpophalangeal joints and extension moment at the distal interphalangeal joints via the extensor mechanism. This extension moment has to be balanced by FDP action. During pressing at proximal phalanges, digit-specific intrinsic muscles are the only ones to play the role

of prime actors (see also Chao et al. 1976; An et al. 1985). Their activation leads to extensor action at more distal finger phalanges that has to be balanced by FDS and FDP. This description does not mention action of finger extensors such as extensor digitorum communis; for now, we can assume that this muscle acts synergistically with the extensor action of the intrinsic muscles. To summarize, while all the mentioned muscle groups are involved in force production at all three sites, their relative involvement is expected to vary with relatively larger forces produced by the prime movers.

While performing the tasks at the three sites of force application, the subjects felt that they were “doing the same”. In addition, the indices of multi-finger synergies showed no significant differences across the three sites: there were comparably strong force-stabilizing synergies and ASAs. While the lack of significant differences across the sites may be considered a statistically weak finding, the number of participants in our study compares favorably with earlier studies of finger interaction and coordination (e.g., Li et al. 1998; Rearick et al. 2003; Winges and Santello 2004; Johnston et al. 2010) and hence we see the study as sufficiently powered to detect effects with moderate-to-large sizes typical of earlier studies with different sites of force production (Li et al. 2001; Shinohara et al. 2003, 2004). Indeed, we saw strongly significant differences between variance components within the two spaces, UCM and ORT, between the two main indices of the motor equivalence analysis (ME and nME), as well as a significant  $\Delta V$  drop in preparation to quick action (ASA, cf. Olafsdottir et al. 2005).

Our observations, taken together with the aforementioned study by Kutch and Valero-Cuevas (2011), suggest that the exact patterns of muscle involvement may limit the range of performance but is unlikely to have a strong effect on digit coordination stabilizing salient performance variables.

### Different indices of force stability within the UCM hypothesis

The UCM hypothesis (Schöner 1995; Scholz and Schöner 1999) is based on the idea that biological systems can modulate stability of various performance variables produced by abundant sets of elemental variables in a task-specific way. This ability is reflected in a number of indices (reviewed in Latash et al. 2007; Latash and Zatsiorsky 2016). The most frequently used ones are the indices of inter-trial variance structure between the two spaces ( $V_{\text{UCM}}$  and  $V_{\text{ORT}}$ ) and indices of motion over time within UCM and ORT (ME and nME). The two sets may be expected to show similar statistical properties. From classical statistics with folded distributions (Leone et al. 1961), inter-trial standard deviations within each of these spaces are expected to be proportional to ME and nME, respectively. Indeed, the data presented here have confirmed the expected correlations between

$\sqrt{V_{UCM}}$  and ME, corroborating two recent studies utilizing cyclical whole-body tasks analyzed at comparable action phases (Falaki et al. 2017; Furmanek et al. 2018). However, in this study, there was no significant correlation between  $\sqrt{V_{ORT}}$  and nME. This last result is unexpected and suggests that performing a quick action may be associated with qualitatively different effects on the motion within the UCM and ORT spaces even when the action requires coming to the same value of the salient performance variable.

The results suggest that the two sets of indices of synergic action,  $V_{UCM}/V_{ORT}$  and  $ME/nME$ , are not redundant, potentially reflecting different neural control processes. The earlier results (Falaki et al. 2017; Furmanek et al. 2018) may be related to the cyclical nature of the used tasks, which may be viewed as a particular case of steady-state action. In discrete actions (see also Mattos et al. 2011), the two groups of indices may behave differently and supply complementary information. This conclusion remains tentative because the mentioned studies differed not only by the type of action, discrete vs. cyclical, but also by the level of analysis (kinetic vs. kinematic vs. electromyographic) and type of tasks (prehension vs. reaching vs. whole-body).

## Concluding comments

We would like to emphasize three important conclusions from our study. First, the experiments showed that stability of action is relatively immune to specific muscle involvement and is likely to reflect interactions among hierarchically higher levels of control. Second, despite use of the distal phalanges for the majority of ecological manipulations, this did not appear to endow them with any obvious advantage over more proximal segments in isometric force production. Finally, our study suggests a distinguishing feature between discrete and cyclical actions (cf. Sternad and Dean 2003; Hogan and Sternad 2007; Friedman et al. 2009) leading to different statistical properties of indices reflecting motion within the corresponding UCM and within ORT. These conclusions need confirmation across tasks and effector systems. We would also like to emphasize that our results fit well the scheme of the neural control of natural actions with a hierarchy using referent coordinates for salient effectors at each of its levels (cf. Latash 2010; Feldman 2015).

**Acknowledgements** The study was in part supported by NIH grant NS095873.

## References

- Ambike S, Zatsiorsky VM, Latash ML (2015) Processes underlying unintentional finger force changes in the absence of visual feedback. *Exp Brain Res* 233:711–721
- Ambike S, Mattos D, Zatsiorsky VM, Latash ML (2016) Synergies in the space of control variables within the equilibrium-point hypothesis. *Neurosci* 315:150–161
- An KN, Chao EY, Cooney WP, Linschield RL (1985) Forces in the normal and abnormal hand. *J Orthop Res* 3:202–211
- Basmajian JV, De Luca CJ (1985) *Muscles Alive*, 5th edn. Williams and Wilkins, Baltimore
- Bernstein NA (1967) *The co-ordination and regulation of movements*. Pergamon Press, Oxford
- Chao EY, Opgrande JD, Axmear FE (1976) Three dimensional force analysis of finger joints in selected isometric hand function. *J Biomech* 19:387–396
- Danion F, Schöner G, Latash ML, Li S, Scholz JP, Zatsiorsky VM (2003) A force mode hypothesis for finger interaction during multi-finger force production tasks. *Biol Cybern* 88:91–98
- Darling WG, Cole KJ, Miller GF (1994) Coordination of index finger movements. *J Biomech* 27:479–491
- Domkin D, Laczko J, Jaric S, Johansson H, Latash ML (2002) Structure of joint variability in bimanual pointing tasks. *Exp Brain Res* 143:11–23
- Falaki A, Huang X, Lewis MM, Latash ML (2017) Motor equivalence and structure of variance: multi-muscle postural synergies in Parkinson's disease. *Exp Brain Res* 235:2243–2258
- Feldman AG (1966) Functional tuning of the nervous system with control of movement or maintenance of a steady posture. II. Controllable parameters of the muscle. *Biophysics* 11:565–578
- Feldman AG (1980) Superposition of motor programs. I. Rhythmic forearm movements in man. *Neurosci* 5:81–90
- Feldman AG (1986) Once more on the equilibrium-point hypothesis ( $\lambda$ -model) for motor control. *J Mot Behav* 18:17–54
- Feldman AG (2015) Referent control of action and perception: challenging conventional theories in behavioral science. Springer, NY
- Friedman J, SKM V, Zatsiorsky VM, Latash ML (2009) The sources of two components of variance: An example of multifinger cyclic force production tasks at different frequencies. *Exp Brain Res* 196:263–277
- Furmanek M, Solnik S, Piscitelli D, Rasouli O, Falaki A, Latash ML (2018) Synergies and motor equivalence in voluntary sway tasks: the effects of visual and mechanical constraints. *J Mot Behav* (in press) <https://doi.org/10.1080/00222895.2017.1367642>
- Gelfand IM, Latash ML (1998) On the problem of adequate language in movement science. *Mot Control* 2:306–313
- Hogan N, Sternad D (2007) On rhythmic and discrete movements: reflections, definitions and implications for motor control. *Exp Brain Res* 181:13–30
- Hughlings Jackson J (1889) On the comparative study of disease of the nervous system. *Brit Med J* 355–362
- Johnston JA, Bobich LR, Santello M (2010) Coordination of intrinsic and extrinsic hand muscle activity as a function of wrist joint angle during two-digit grasping. *Neurosci Lett* 474:104–108
- Kang N, Shinohara M, Zatsiorsky VM, Latash ML (2004) Learning multi-finger synergies: an uncontrolled manifold analysis. *Exp Brain Res* 157:336–350
- Kutch JJ, Valero-Cuevas FJ (2011) Muscle redundancy does not imply robustness to muscle dysfunction. *J Biomech* 44:1264–1270
- Landsmeer JMF, Long C (1965) The mechanism of finger control, based on electromyograms and location analysis. *Acta Anat* 60:330–347
- Latash ML (2008) *Synergy*. Oxford University Press, New York

- Latash ML (2010) Motor synergies and the equilibrium-point hypothesis. *Mot Control* 14:294–322
- Latash ML (2012) The bliss (not the problem) of motor abundance (not redundancy). *Exp Brain Res* 217:1–5
- Latash ML (2016) Towards physics of neural processes and behavior. *Neurosci Biobehav Rev* 69:136–146
- Latash ML (2017) Biological movement and laws of physics. *Mot Control* 21:327–344
- Latash ML, Zatsiorsky VM (1993) Joint stiffness: myth or reality? *Hum Move Sci* 12:653–692
- Latash ML, Zatsiorsky VM (2016) *Biomechanics and motor control: defining central concepts*. Academic Press, New York, NY
- Latash ML, Scholz JF, Danion F, Schöner G (2001) Structure of motor variability in marginally redundant multi-finger force production tasks. *Exp Brain Res* 141:153–165
- Latash ML, Scholz JF, Danion F, Schöner G (2002) Finger coordination during discrete and oscillatory force production tasks. *Exp Brain Res* 146:412–432
- Latash ML, Shim JK, Smilga AV, Zatsiorsky V (2005) A central back-coupling hypothesis on the organization of motor synergies: a physical metaphor and a neural model. *Biol Cybern* 92:186–191
- Latash ML, Scholz JP, Schöner G (2007) Toward a new theory of motor synergies. *Mot Control* 11:275–307
- Leone FC, Nottingham RB, Nelson LS (1961) The folded normal distribution. *Technometrics* 3:543–550
- Li ZM, Latash ML, Zatsiorsky VM (1998) Force sharing among fingers as a model of the redundancy problem. *Exp Brain Res* 119:276–286
- Li ZM, Zatsiorsky VM, Latash ML (2000) Contribution of the extrinsic and intrinsic hand muscles to the moments in finger joints. *Clin Biomech* 15:203–211
- Li S, Danion F, Latash ML, Li Z-M, Zatsiorsky VM (2001) Bilateral deficit and symmetry in finger force production during two-hand multi-finger tasks. *Exp Brain Res* 141:530–540
- Li Z-M, Zatsiorsky VM, Latash ML, Bose NK (2002) Anatomically and experimentally based neural networks modelling force coordination in static multi-finger tasks. *Neurocomputing* 47:259–275
- Long C (1965) Intrinsic-extrinsic muscle control of the fingers. *J Bone Joint Surg* 50A:973–984
- Martin V, Scholz JP, Schöner G (2009) Redundancy, self-motion, and motor control. *Neural Comput* 21:1371–1414
- Mattos D, Latash ML, Park E, Kuhl J, Scholz JP (2011) Unpredictable elbow joint perturbation during reaching results in multijoint motor equivalence. *J Neurophysiol* 106:1424–1436
- Olafsdottir H, Yoshida N, Zatsiorsky VM, Latash ML (2005) Anticipatory covariation of finger forces during self-paced and reaction time force production. *Neurosci Lett* 381:92–96
- Rearick MP, Casares A, Santello M (2003) Task-dependent modulation of multi-digit force coordination patterns. *J Neurophysiol* 89:1317–1326
- Reschechtko S, Latash ML (2017) Stability of hand force production: I. Hand level control variables and multi-finger synergies. *J Neurophysiol* 118:3152–3164
- Schieber MH, Santello M (2004) Hand function: peripheral and central constraints on performance. *J Appl Physiol* 96:2293–2300
- Scholz JP, Schöner G (1999) The uncontrolled manifold concept: identifying control variables for a functional task. *Exp Brain Res* 126:289–306
- Scholz JP, Danion F, Latash ML, Schöner G (2002) Understanding finger coordination through analysis of the structure of force variability. *Biol Cybern* 86:29–39
- Schöner G (1995) Recent developments and problems in human movement science and their conceptual implications. *Ecol Psychol* 8:291–314
- Shaklai S, Minouni-Blouch A, Levin M, Friedman J (2017) Development of finger force coordination in children. *Exp Brain Res* 235:3709–3720
- Shim JK, Olafsdottir H, Zatsiorsky VM, Latash ML (2005) The emergence and disappearance of multi-digit synergies during force production tasks. *Exp Brain Res* 164:260–270
- Shinohara M, Latash ML, Zatsiorsky VM (2003) Age effects on force production by the intrinsic and extrinsic hand muscles and finger interaction during maximal contraction tasks. *J Appl Physiol* 95:1361–1369
- Shinohara M, Scholz JP, Zatsiorsky VM, Latash ML (2004) Finger interaction during accurate multi-finger force production tasks in young and elderly persons. *Exp Brain Res* 156:282–292
- Slobounov S, Chiang H, Johnston J, Ray W (2002) Modulated cortical control of individual fingers in experienced musicians: an EEG study. *Electroencephalographic study*. *Clin Neurophysiol* 113:2013–2024
- Solnik S, Pazin N, Coelho CJ, Rosenbaum DA, Scholz JP, Zatsiorsky VM, Latash ML (2013) End-state comfort and joint configuration variance during reaching. *Exp Brain Res* 225(3):431–442
- Sternad D, Dean WJ (2003) Rhythmic and discrete elements in multi-joint coordination. *Brain Res* 989:152–171
- Vaillancourt DE, Russell DM (2002) Temporal capacity of short-term visuomotor memory in continuous force production. *Exp Brain Res* 145:275–285
- Winges SA, Santello M (2004) Common input to motor units of digit flexors during multi-digit grasping. *J Neurophysiol* 92:3210–3220
- Wu Y-H, Latash ML (2014) The effects of practice on coordination. *Exer Sport Sci Rev* 42:37–42
- Xu J, Ejaz N, Hertler B, Branscheidt M, Widmer M, Faria AV, Harran MD, Cortes JC, Kim N, Celnik PA, Kitago T, Luft AR, Krakauer JW, Diedrichsen J (2017) Separable systems for recovery of finger strength and control after stroke. *J Neurophysiol* 118:1151–1163
- Zatsiorsky VM, Latash ML (2008) Multi-finger prehension: an overview. *J Mot Behav* 40:446–476
- Zatsiorsky VM, Li Z-M, Latash ML (1998) Coordinated force production in multi-finger tasks: finger interaction and neural network modeling. *Biol Cybern* 79(2):139–150
- Zatsiorsky VM, Li ZM, Latash ML (2000) Enslaving effects in multi-finger force production. *Exp Brain Res* 131:187–195